Atomic-Scale Assessment of First-Wall Materials for Fusion Reactors: Insights and Challenges for Materials Simulations

Emily A. Carter
School of Engineering and Applied Science
Princeton University
http://carter.princeton.edu

Fusion energy challenges: plasma control and materials

Problem: Materials experiments mostly post-mortem

Need efficient, accurate materials simulations of *in-situ* phenomena

Materials for Fusion Reactor Walls

Two classes of candidates for plasma-facing components:

1. **solid:** tungsten

Advantage:
High melting point
Redeposition after sputtering
Disadvantage:
neutron damage
erosion

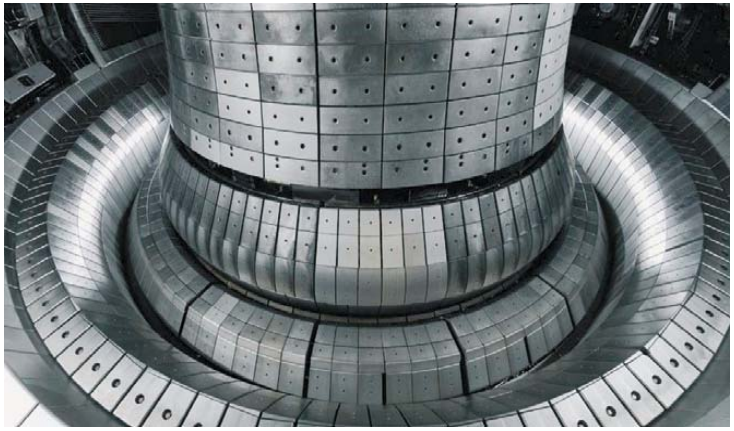

ASDEX in full tungsten configuration (Garching)

2. **liquids:** lithium, tin, gallium, etc.

Advantage:
no irreversible erosion
no neutron damage
no heat overload

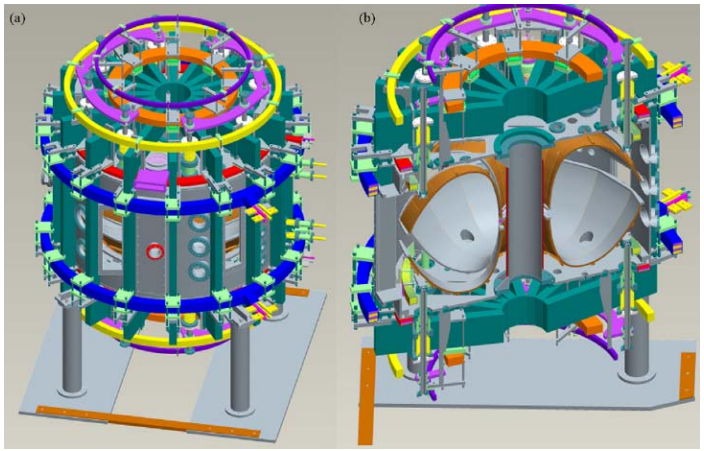

Lithium Tokamak Experiment (LTX)
Princeton Plasma Physics Laboratory

Materials Properties from Quantum Mechanics: Density Functional Theory

$$E_{DFT}[\rho(\vec{r})] = T_S[\rho(\vec{r})] + J_{ee}[\rho(\vec{r})] + E_{XC}[\rho(\vec{r})] + \int V_{ext}(\vec{r})\rho(\vec{r})dr^3$$

How to accurately simulate matter without wavefunctions?
Challenges: electron kinetic energy and electron-ion interaction

In Kohn-Sham DFT

$$T_S[\rho(\vec{r})] = -\frac{1}{2}\sum_{i=occ}\int \psi_i^*(\vec{r})\nabla^2\psi_i(\vec{r})dr^3$$

$$\rho(\vec{r}) = \sum_i f_i\psi_i^*(\vec{r})\psi_i(\vec{r})$$

(1) Introduce orbitals. Must orthogonalize.

(2) Computational cost is usually ~ $O(N_{basis}*N_{orb}^2)$.

(3) Linear-scaling KS-DFT: localized basis sets or locally truncated KS equations → large prefactor & not applicable to metals.

In Orbital-Free DFT

$$T_{TF} = \frac{3}{10}\left(3\pi^2\right)^{2/3}\int \rho^{5/3}(\vec{r})dr^3$$

Thomas-Fermi kinetic energy density functional (KEDF)

$$T_{vW} = \frac{1}{8}\int \frac{|\nabla\rho(\vec{r})|^2}{\rho(\vec{r})}dr^3$$

von Weizsäcker KEDF

(1) Basic variable is the electron density.

(2) Computational cost can be made to scale as ~O(N ln N).

(3) Local and semilocal KEDFs not accurate => Improve accuracy by adding nonlocal term.

Orbital-Free DFT concerns: kinetic and electron-ion energies

$$E_{OF-DFT}[\rho(\vec{r})] = T_S[\rho(\vec{r})] + J_{ee}[\rho(\vec{r})] + E_{XC}[\rho(\vec{r})] + \int V_{ext}(\vec{r})\rho(\vec{r})dr^3$$

Quick history of Carter group contributions:

1999 – nonlocal KEDF with density-dependent kernel for *main group metals* (Y. Wang, N. Govind, EAC, PRB **60**, 16350 (1999)). WGC99: KSDFT accuracy, orders of magnitude faster

$$T_S = T_{TF} + T_{vW} + T_{nonlocal}$$

$$T_{nonlocal} = \iint \rho^{\alpha}(\vec{r})\Omega(\vec{r};\vec{r}')\rho^{\beta}(\vec{r}')dr^3dr'^3$$

$$\frac{1}{\tilde{\chi}(\mathbf{q})} = -\tilde{F}\left(\frac{\delta^2 T_s[\rho]}{\delta\rho(\mathbf{r})\delta\rho(\mathbf{r}')}\right)$$

2004 – KS-OEP-based bulk-derived local pseudopotentials for electron-ion interactions (B. Zhou, Y. A. Wang, and EAC *Phys. Rev. B*, **69** 125109 (2004))

2009 – Fully linear scaling (in ions and electrons) code with small prefactor via FFT/PME (L. Hung and EAC, *Chem. Phys. Lett. Frontier Article*, **475**, 163 (2009)): 1M atom benchmarks, science w/O(10^4) atoms

2010 – HC10 nonlocal KEDF for *covalent materials* (C. Huang and EAC, *Phys. Rev. B* **81**, 045206 (2010))

2012 – HC10 KEDF applied to *molecules* (J. Xia, C. Huang, I. Shin, and EAC, *J. Chem. Phys.* **136**, 084102 (2012))

2012 – Density-decomposed nonlocal KEDFs for *transition metals and semiconductors* (C. Huang and EAC, *Phys. Rev. B* **85**, 045126(2012); J. Xia and EAC, *Phys. Rev. B* **86**, 235109 (2012); MSMSE **24**, 035014 (2016).)

2013 - *Transition metals* via angular-momentum-dependent OFDFT (Y. Ke, F. Libisch, J. Xia, L.-W. Wang, and EAC, *Phys. Rev. Lett.* **111**, 066402 (2013); Y. Ke, F. Libisch, J. Xia, and E. A. Carter, *Phys. Rev. B*, **89**, 155112 (2014))

2014 – Enhanced von Weizsäcker WGC KEDF for *semiconductors* (I. Shin and EAC, *J. Chem. Phys.*, **140**, 18A531 (2014)) 2015 – Self-consistent GGA KEDF (J. Xia and EAC, *Phys. Rev. B*, **91**, 045124; **92**, 117102 (2015))

2016 – Petascale Small Box FFT OFDFT (M. Chen, X. Jiang, H. Zhuang, L. Wang, EAC, *J. Chem. Theor. Comp.*, **12**, 2950 (2016)) ■PROFESS 3.0 free download, http://www.princeton.edu/carter/research/software/

H Isotope Adsorption on W(110) and W(001) Surfaces

- W: bcc
- Several low-energy surfaces
- (110) & (001) well-characterized experimentally

$E_{ads} = E(H/W) - \frac{1}{2} E(H_2) - E(W)$
from Kohn-Sham DFT

W(110)
Hollow site
E_{ads} = -0.75 eV

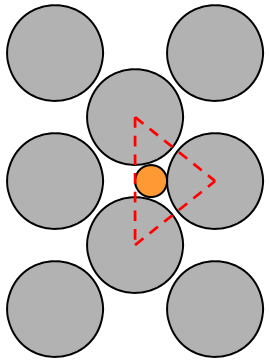

W(110)
adsorption on 3-fold site

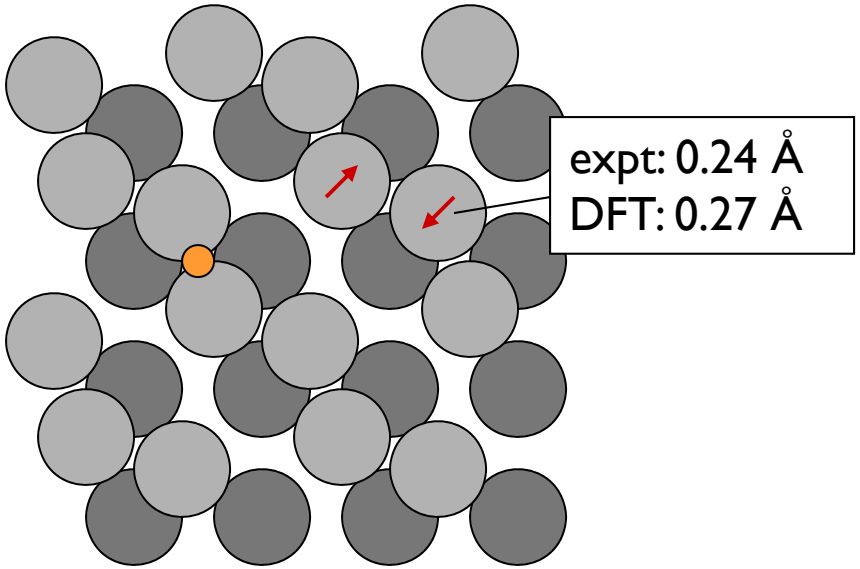

W(001)-reconstruction
adsorption on short-bridge site

W(001)
- E_{ads} = -0.92 eV

Surface diffusion barrier: ~0.50 eV

- **H prefers high-coordination sites**
- **Exothermic dissociative adsorption**

D. F. Johnson and E. A. Carter, *J. Mater. Res.*, **25**, 315 (2010).

Energy Barriers for H Incorporation in Pristine W

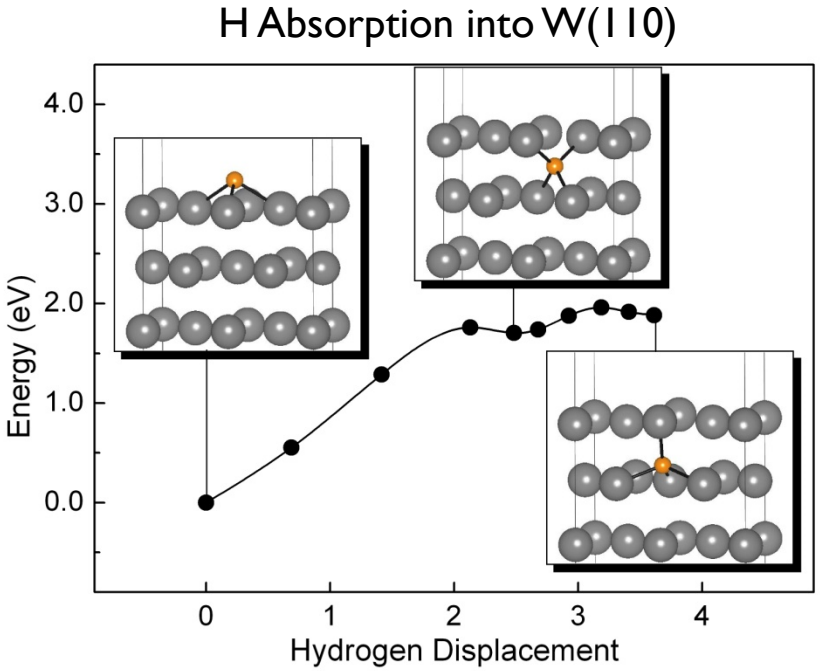

Surface-to-subsurface diffusion

- Very endothermic
- Energy barriers > 1.2 eV

Overall Path:

Surface → subsurface → deeper site

- MEP for W(110): 1.94 eV
- MEP for W(001):
  - SB → sub-subsurface: 2.13 eV
  - SB → LB → sub-subsurface: **2.08 eV**
- Outward barriers < 0.2 eV

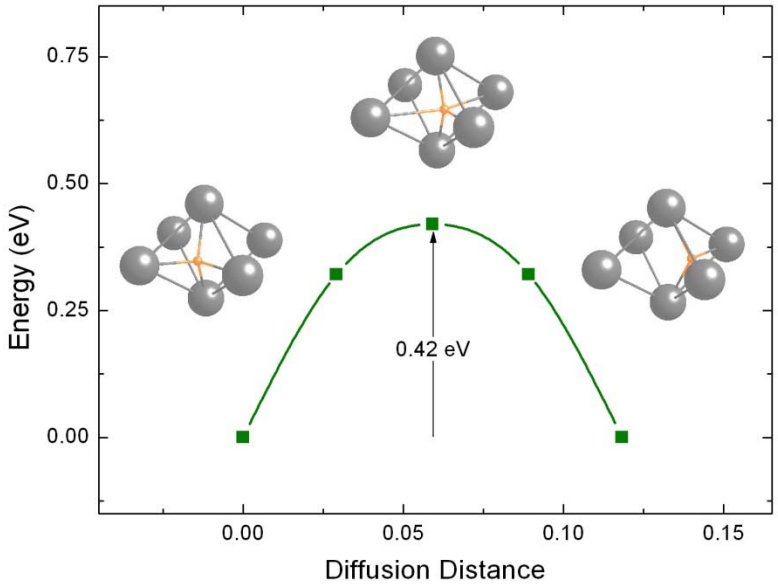

Bulk Diffusion

- H diffuses via tetrahedral sites
- Bulk Diffusion Barrier: **0.42 eV**
  - similar to 2nd absorption step

- **Large energy barriers to absorption**
- **H readily diffuses outward to surface**
- **Fairly large bulk diffusion barrier**

D. F. Johnson and E. A. Carter, *J. Mater. Res.*, **25**, 315 (2010).

H Isotope Trapping at Vacancies in W

High energy particle flux
- Damage to subsurface layers/bulk
- Vacancy formation
- H binds exothermically
- Up to six H atoms will bind to vacancy

Perfect bulk dissolution energy
E_s = 0.96 eV

H sits at octahedral site near vacancy

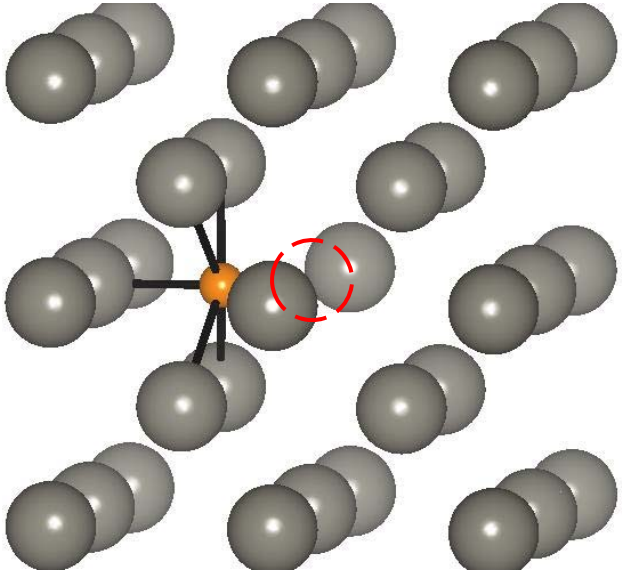

H-W_{53}V

$$E_{Bind}(H) = E(W_{53}VH_n) + E(W_{54}) - E(W_{53}VH_{n-1}) - E(W_{54}H)$$

final initial

VH_n	Binding	E_{Bind}(H) eV
V	$W_{54} \rightarrow W_{53}V$	**3.32**
1	$V+H \rightarrow VH$	**-1.24**
2	$VH+H \rightarrow VH_2$	**-1.24**
3	$VH_2+H \rightarrow VH_3$	**-1.12**
4	$VH_3+H \rightarrow VH_4$	**-1.00**
5	$VH_4+H \rightarrow VH_5$	**-0.94**
6	$VH_5+H \rightarrow VH_6$	**-0.54**

H stabilizes vacancies, $E_{Bind}(3H) > -E_F(Vac)$

D. F. Johnson and E. A. Carter, *J. Mater. Res.*, **25**, 315 (2010).

Hydrogen-Enhanced Decohesion

Born-Haber cycle:

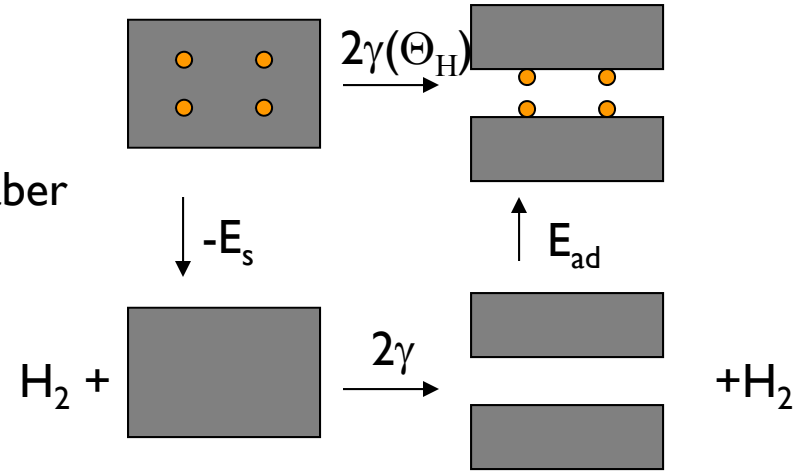

$$2\gamma(\Theta_H) = -E_s + 2\gamma(0) + E_{ad}(\Theta_H)$$

- Normalize γ w.r.t surface area
- Well-defined quantities: E_s, γ, E_{ad}

Assumptions

- H diffuses quickly from bulk to surface
- E_s does not vary with H concentration

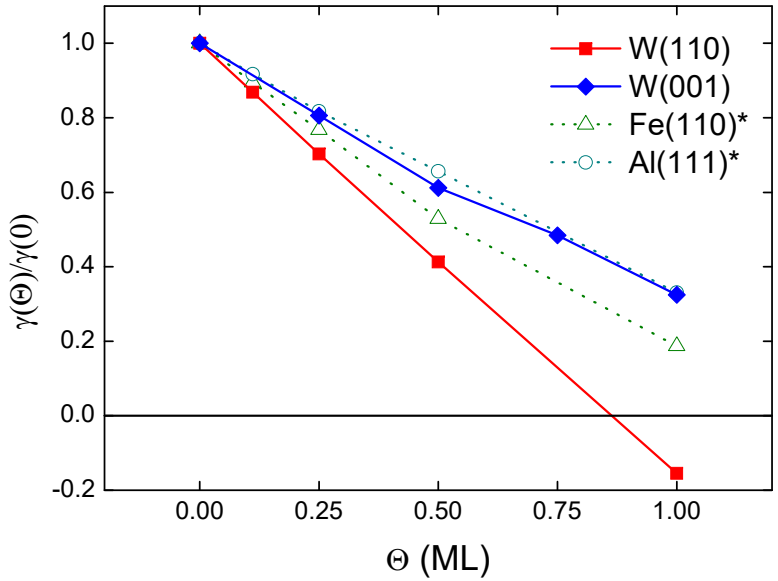

- **H stabilizes W surfaces**
- HED is more pronounced in W than Fe and Al

*D.E. Jiang and E.A. Carter, Acta Mater. **52** (2004) 4801

D. F. Johnson and E. A. Carter, *J. Mater. Res.*, **25**, 315 (2010).

H isotopes on and in pristine and defective W

- Exothermic adsorption
- Endothermic absorption for perfect bulk W
- Large barriers for absorption
- Outward diffusion barriers ~ 0
- Vacancies trap up to six H atoms

E_s ~ 1 eV → H destabilized in bulk
E_{ads} ~ -1 eV → H stabilized at surfaces

H-Enhanced Decohesion

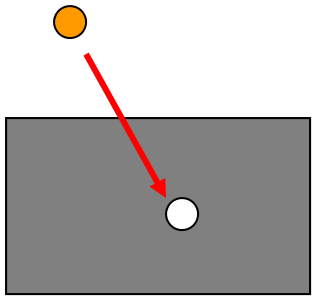

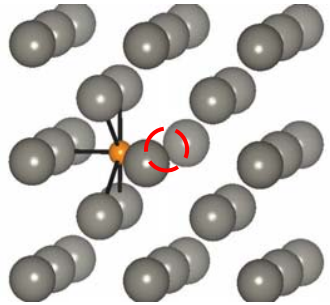

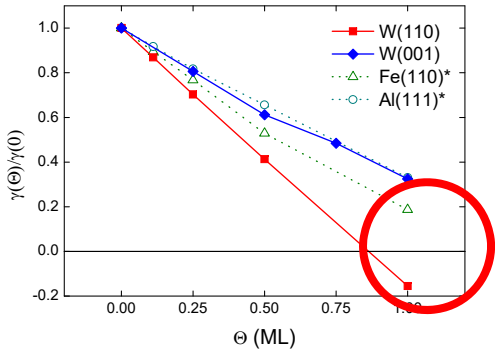

Vacancy formation → H clusters near vacancies → Decohesion → Cracking/Blistering

- **Need careful control of temperature gradient**
- **Promote vacancy-interstitial annihilation in high damage regions**
- **Promote H isotope diffusion to surface/desorption**

D. F. Johnson and E. A. Carter, *J. Mater. Res.*, **25**, 315 (2010).

From atoms to tokamaks project

- Our vision: atoms to thin film flows

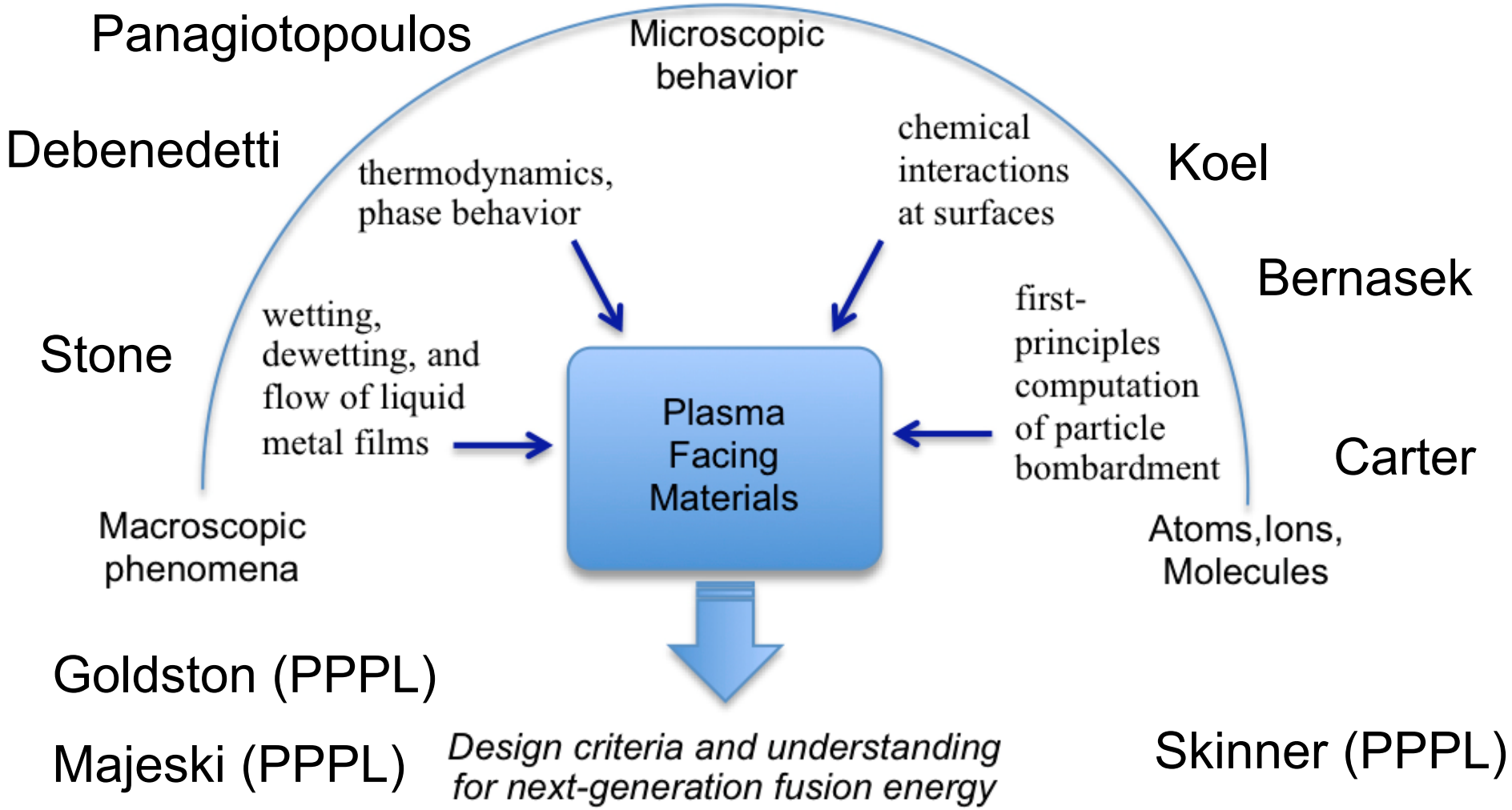

Scientific questions to address

- Describe and understand fluid dynamics relevant capillary pore systems and to liquid metal-wall configurations, including responses to localized large heat and particle fluxes, possible dewetting and rewetting scenarios, influence of thermocapillary and MHD forces, and how these coupled processes are influenced by changes in the surface chemistry
- Measure and characterize surface processes that control D recycling: D uptake (sorption) rates and influence of impurities; how fast deposited D diffuses into the bulk; concentration nucleating deuteride phase; and interfacial effects impacting flow including O and C impurities
- Develop theory and simulations to extend the limited material data (wetting, flow, and solubility) and predict bulk and surface properties of liquid metals relevant to fusion energy conditions
- Determine the conditions that produce deuteride formation during the interaction of the plasma (D) with liquid metals

Assessment of Liquid Metal Films via Density Functional Theory Dynamics

$$E_{etot}^{OFDFT}[\rho] = T_S^{OFDFT}[\rho] + E_{Hart}[\rho] + E_{XC}[\rho] + \int V_{ext}^{local}(\mathbf{r})\rho(\mathbf{r})d\mathbf{r}$$

Massively parallel, linear scaling QM method for millions of atoms

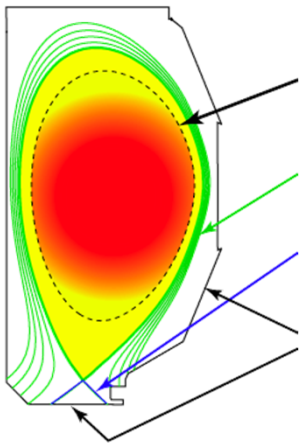

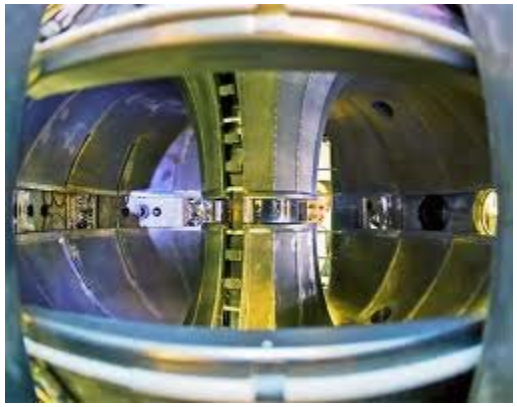

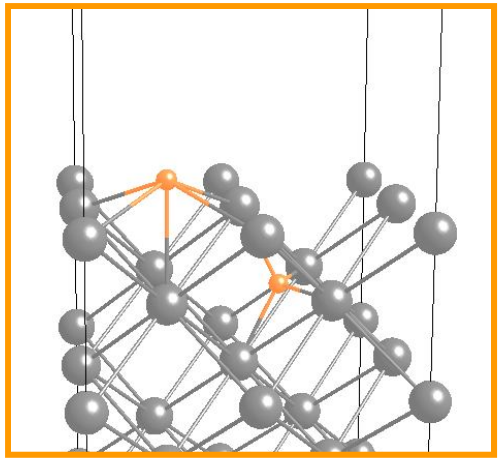

Consider liquid lithium as first wall material

Goal: Understand deuterium/tritium bombardment of liquid Li films

Liquid Li: Theory versus Experiment

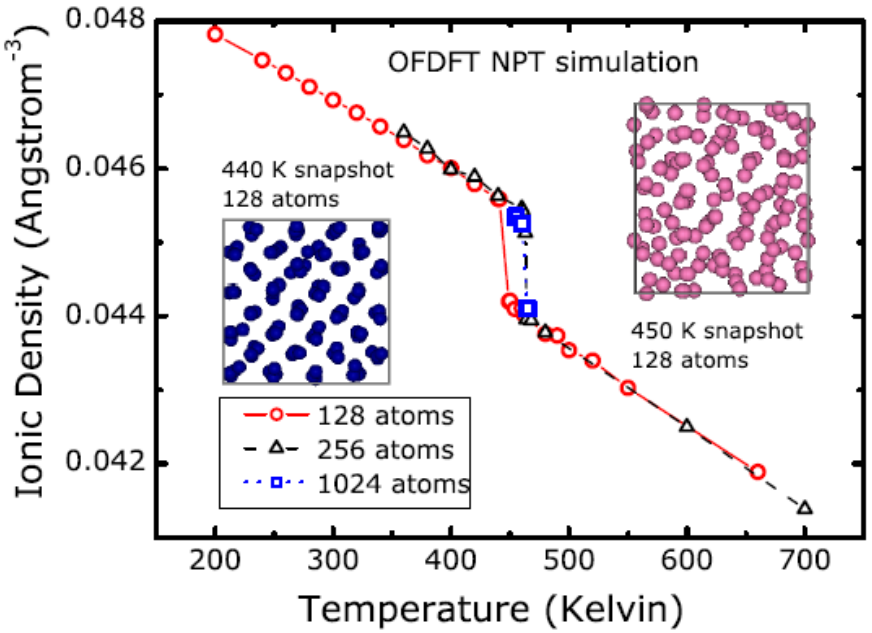

OFDFT-MD heating melting point: **465 K**
Refined coexistence melting point: **442 K**
Experimental melting point: **453 K**
(R. Boehler, Phys. Rev. B. 27, 6754 (1983))

$$g(r) = \frac{1}{\rho N}\langle \sum_{i=1}^{N} \sum_{j=1, j\neq i}^{N} \delta(\mathbf{r} - \mathbf{R_i} + \mathbf{R_j}) \rangle \qquad S(k) = \frac{1}{N}\langle \sum_{i=1}^{N} \sum_{j=1}^{N} e^{i\mathbf{k}(\mathbf{R_i} - \mathbf{R_j})} \rangle$$

OFDFT-NPT-MD and experimental g(r), S(k) match nearly perfectly at two different temperatures.

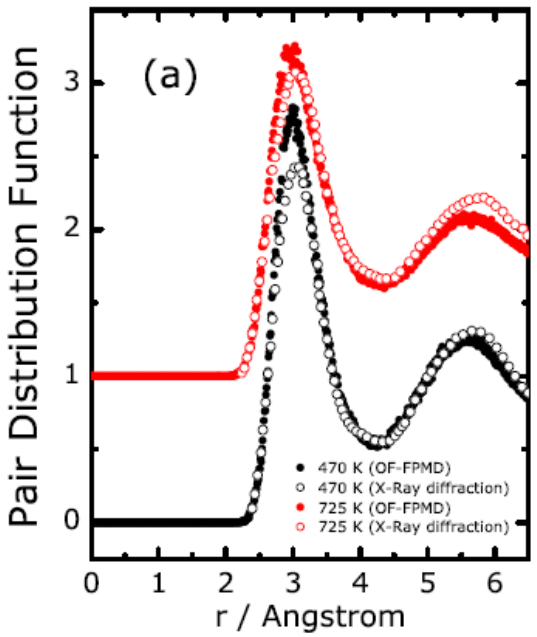

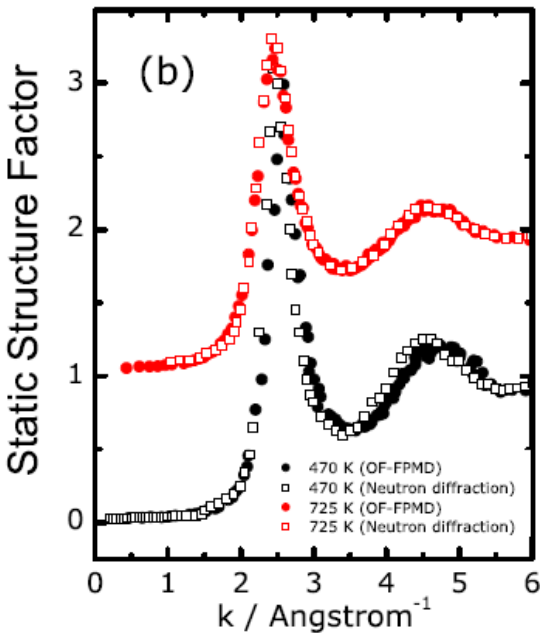

M. Chen, L. Hung, C. Huang, J. Xia, and EAC, Mol. Phys. 111, 3448 (2013).

Viscosity and Surface Tension of Liquid Li

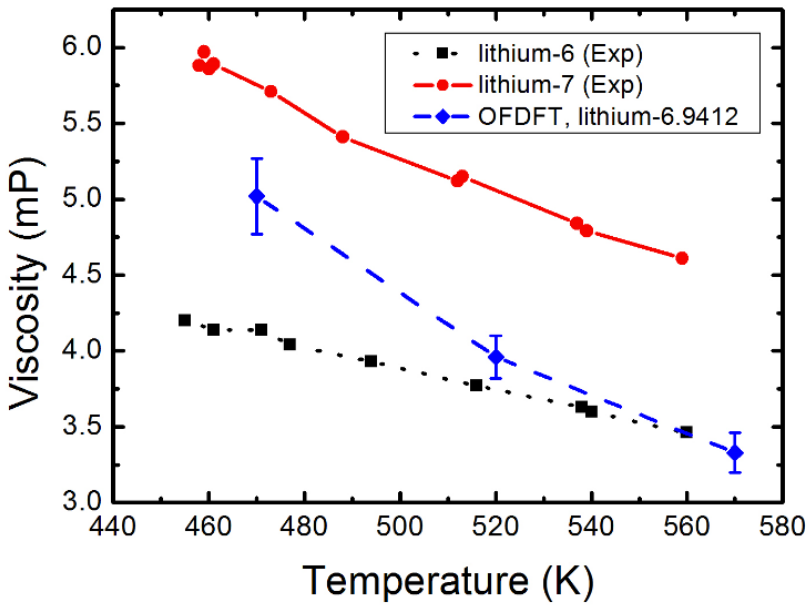

Surface tension (mN/m)	*453 K (melting point)*	*470 K*	*520 K*	*570 K*
OFDFT-MD		***364***	***345***	***339***
Experiment	***398 [1]***	***trend: decreasing***		

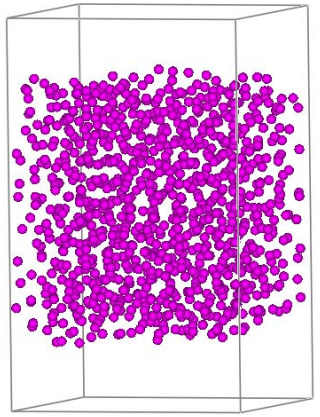

[1] Phys. Rev. **128**, 6 (1962)

Mohan Chen, Joseph R. Vella, Frank H. Stillinger, Emily A. Carter, Athanassios Z. Panagiotopoulos, Pablo G. Debenedetti, AIChE Journal, **6**, 2841(2015).

D atoms bombarding Li surfaces

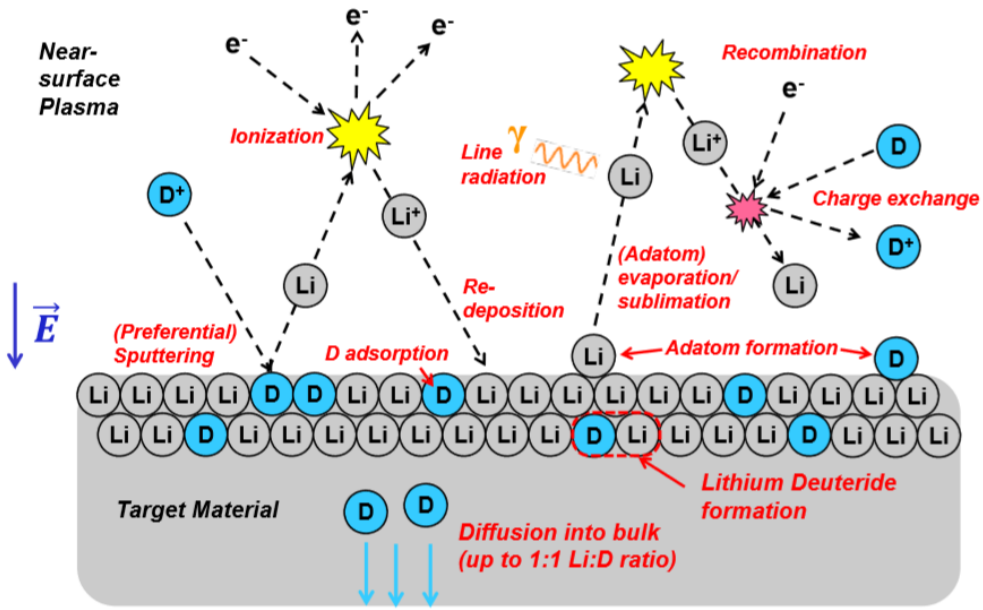

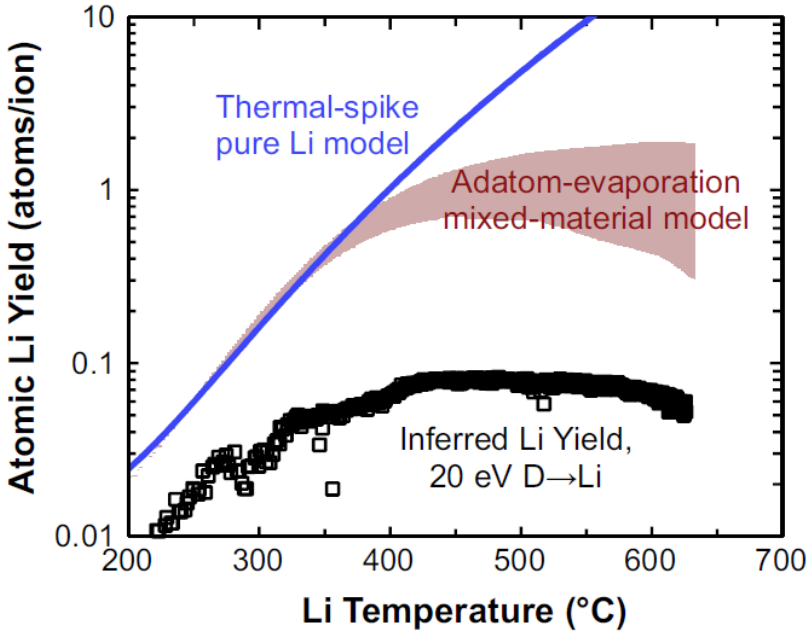

T. Abrams, et al. J. Nucl. Mater. vol. 463, p.1169 (2015)

- **Li sputtering yield and vapor pressure limit max operating T of fusion reactor.**
- **Low D flux experiments suggested max T possible may be too low for practical operation (Phys. Rev. B 76, 205434 (2007)).**

- **High D flux experiment.**
- **Li sputtering yield 5-10 times smaller than expected, suggesting max operating T for liquid Li could be higher than previously thought.**
- **Hypothesis: LiD may form due to the high-concentration D in liquid Li.**

Question:

When D atoms in liquid Li exceed solubility limit, what happens?

Phase diagram of Li/LiD

- x: mole fraction LiD
- alpha-phase: enriched in Li.
- beta-phase: enriched in LiD.

- Below 958 K, solid LiD in liquid Li should nucleate.
- Origin of reduced sputtering, higher T survival of wall?

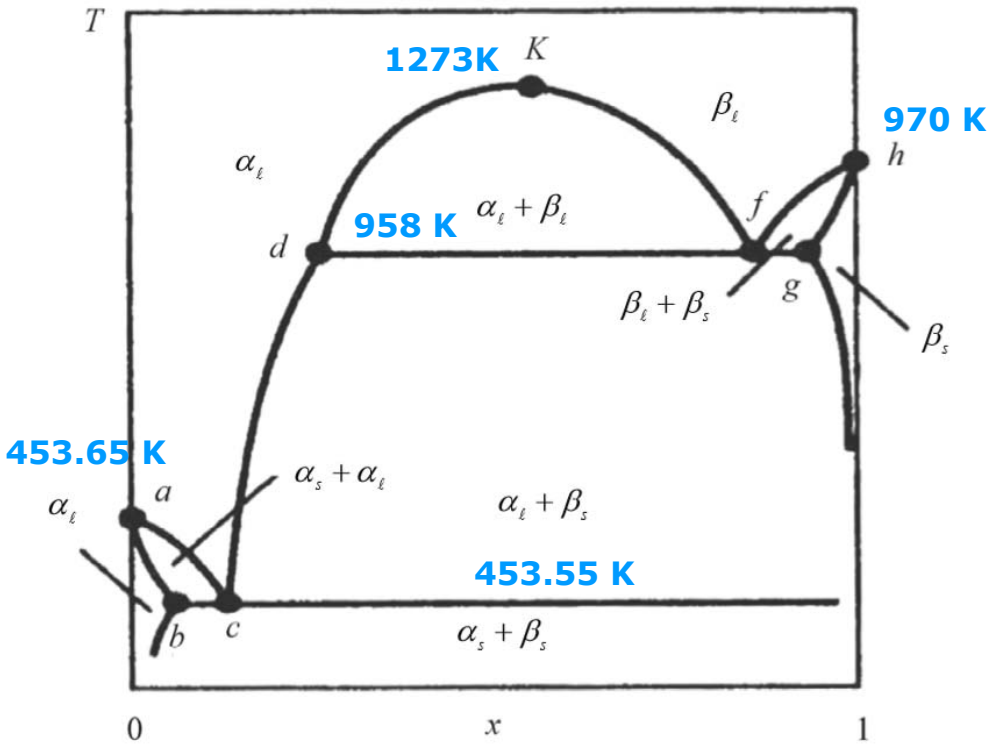

Table 1. Characteristic points of the temperature composition diagram for the Li-LiH system.

Coordinates	*a*	*b*	*c*	*d*	*κ*	*f*	*g*	*h*
T, *K*	453.65	453.55	453.55	958	1273	958	958	970
x	0	0.56×10^{-4}	1.6×10^{-4}	0.26	0.60	0.98	0.99	1

Open Journal of Physical Chemistry, 2012, 2, 141-146

Li-H/D: Challenging for OFDFT MD Simulations

- Different H adsorption sites on Li (100)

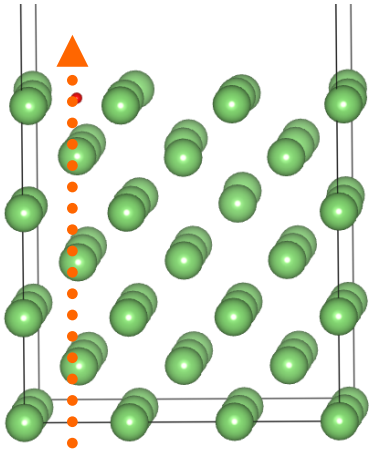

Hollow site H

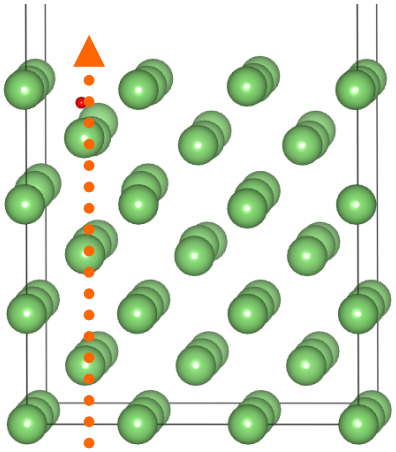

Bridge H

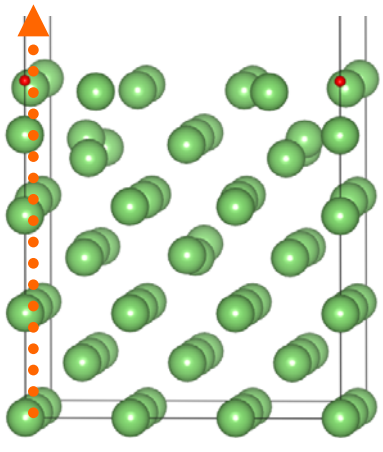

Top H

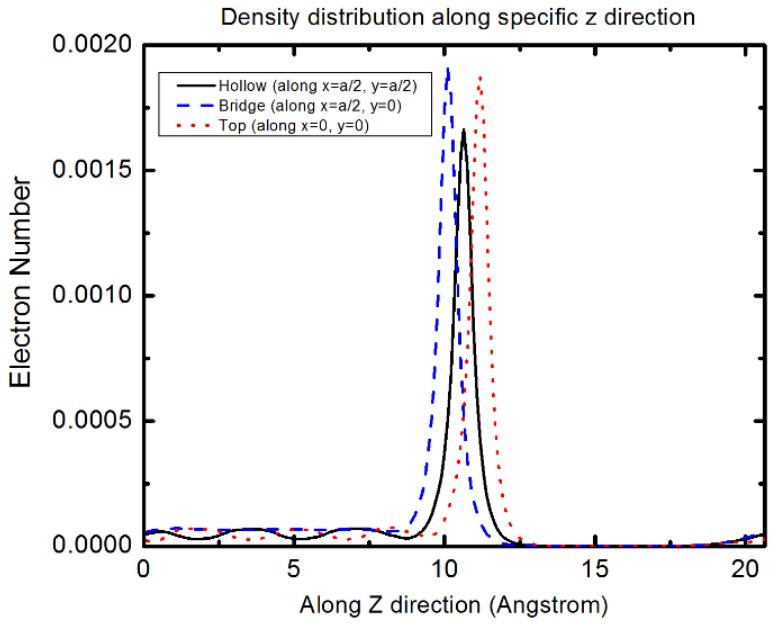

- Electron density of hydrogen is highly localized.
- Our nonlocal KEDFs based on Lindhard response are not appropriate for localized densities.
- Density decomposed KEDFs not accurate enough.
- Resort to KSDFT-MD until new KEDFs or new hybrid formalism fully developed.

KSDFT-MD of solid and liquid Li and LiD

	KSDFT-MD Melting T	Expt Melting T
Li	**between 400 and 470 K**	**453 K**
LiD	**between 943 and 1143 K**	**960 K**

- **Static structure factors of Li**

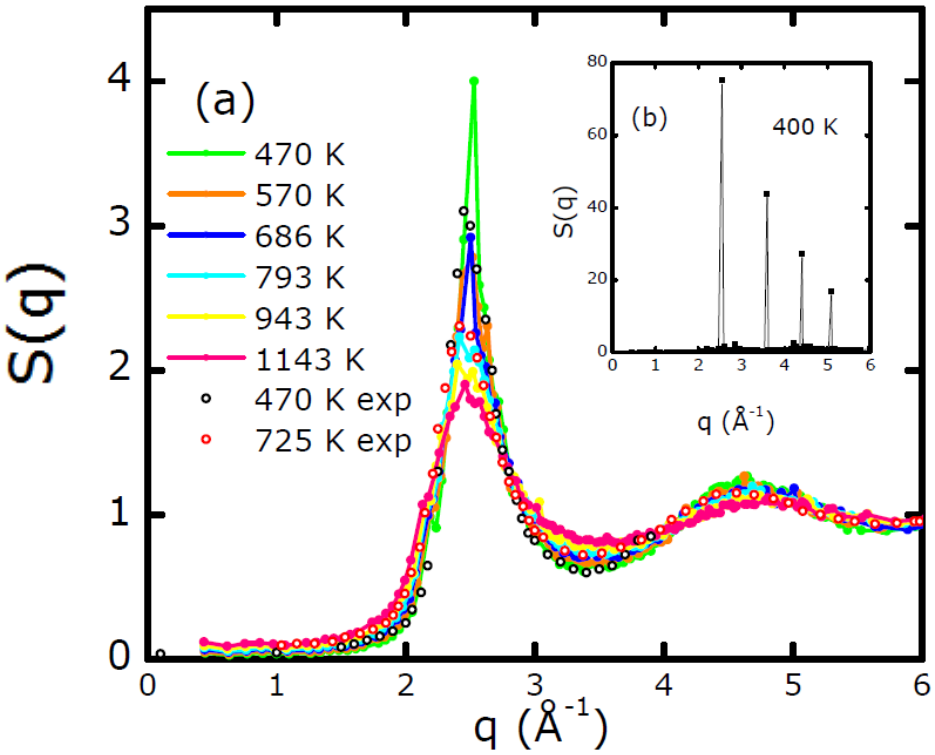

- **Partial pair distribution functions of LiD**

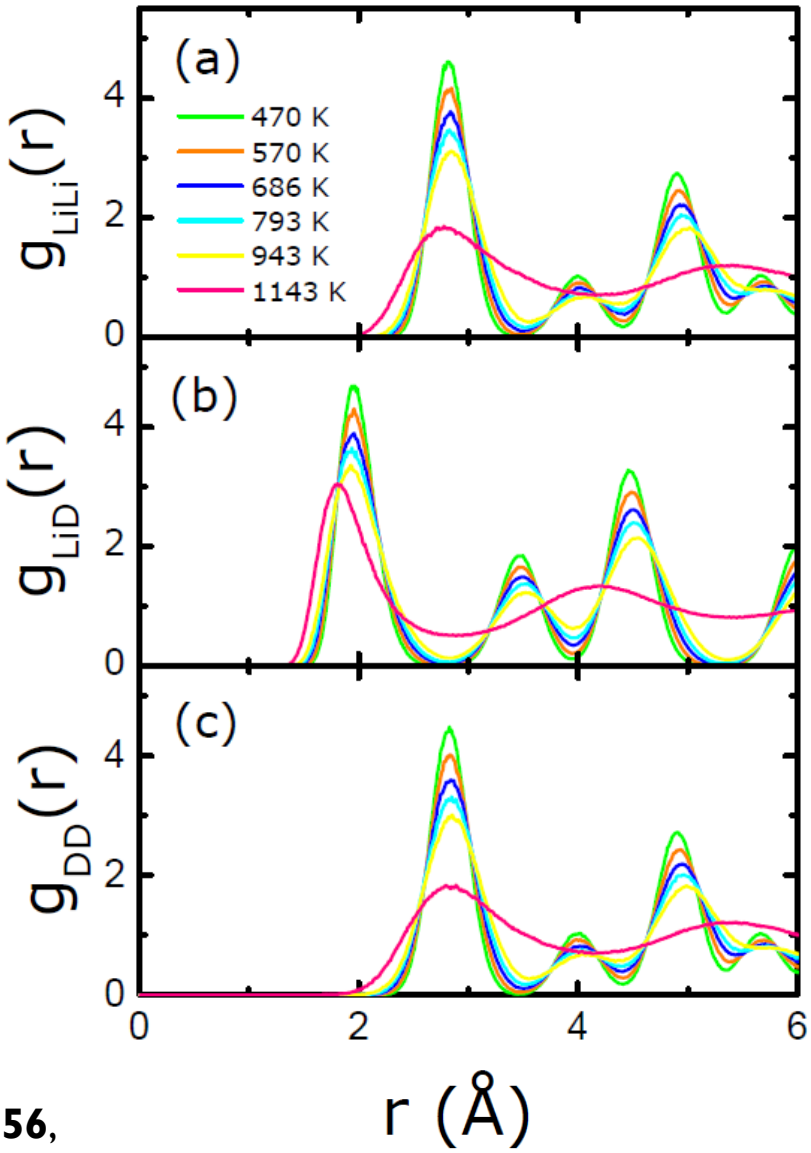

M. Chen, T. Abrams, M. Jaworski, E. A. Carter, *Nuclear Fusion,* **56**, 016020 (2016).

Bond angles in Li bcc and LiD rock-salt structures

- **Li bcc:**

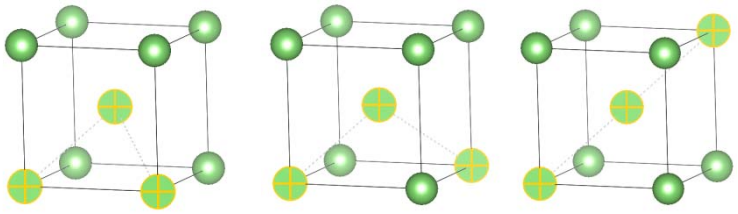

70.5° **109.5°** **180°**

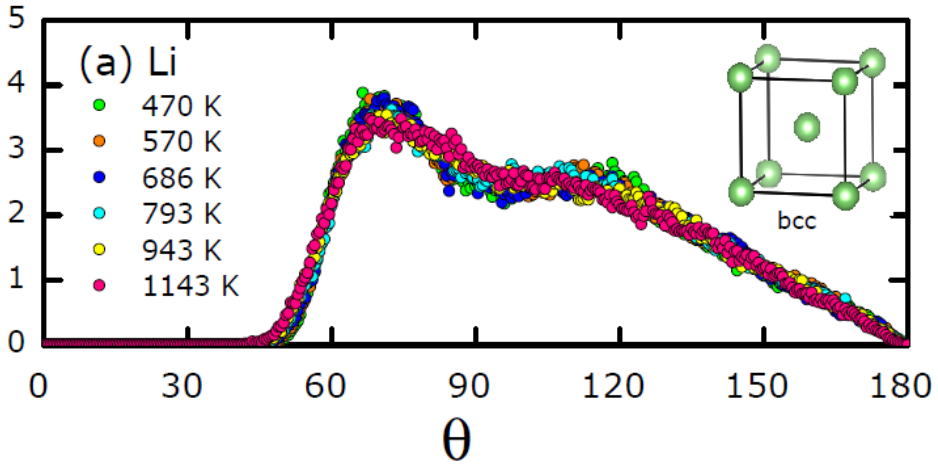

- **LiD rock-salt:**

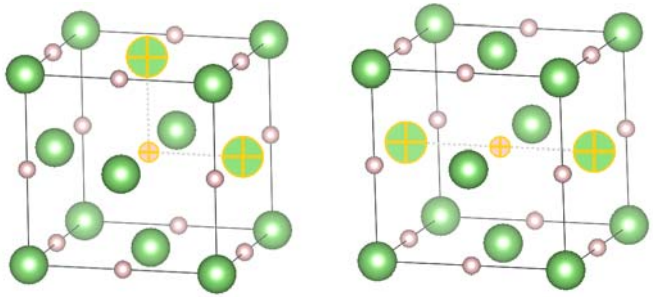

90° **180°**

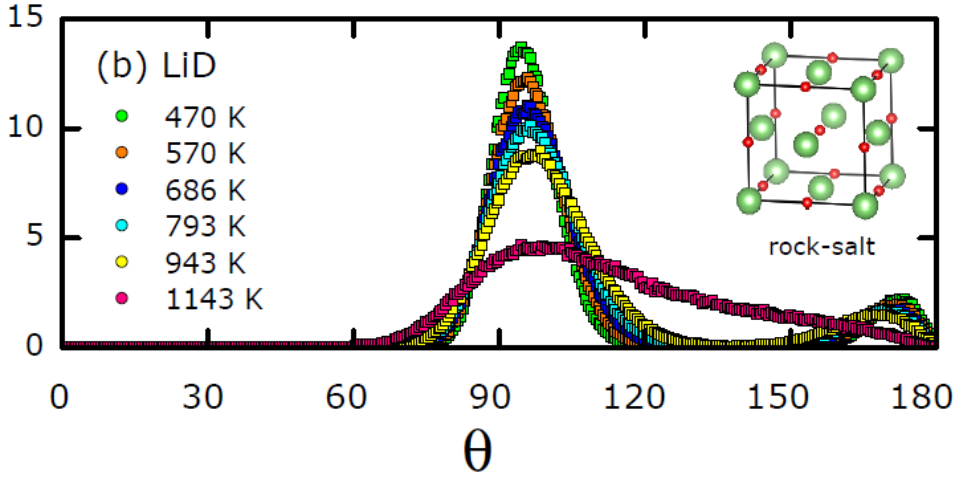

1) Liquid Li and LiD have specific local structures.
2) Bond angle distribution function is a fingerprint to identify these local structures.

M. Chen, T. Abrams, M. Jaworski, E. A. Carter, *Nuclear Fusion,* **56**, 016020 (2016).

Liquid Li with inserted D atoms *above* the melting point of LiD

- **Inserted D atoms into liquid Li (heated up to 1500 K and then quenched down to target temperatures).**
- **1143 K: mixture of liquid Li and LiD.**

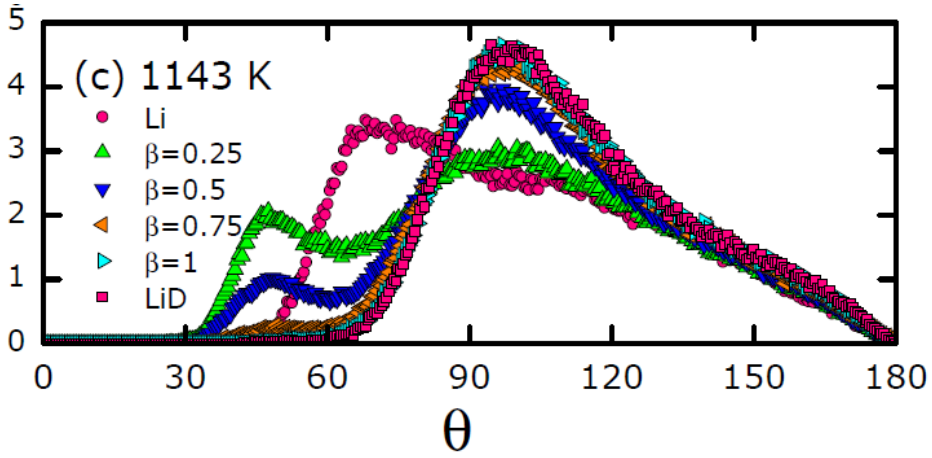

- **β: ratio between D and Li atoms.**
- **Partial bond angle distribution functions.**

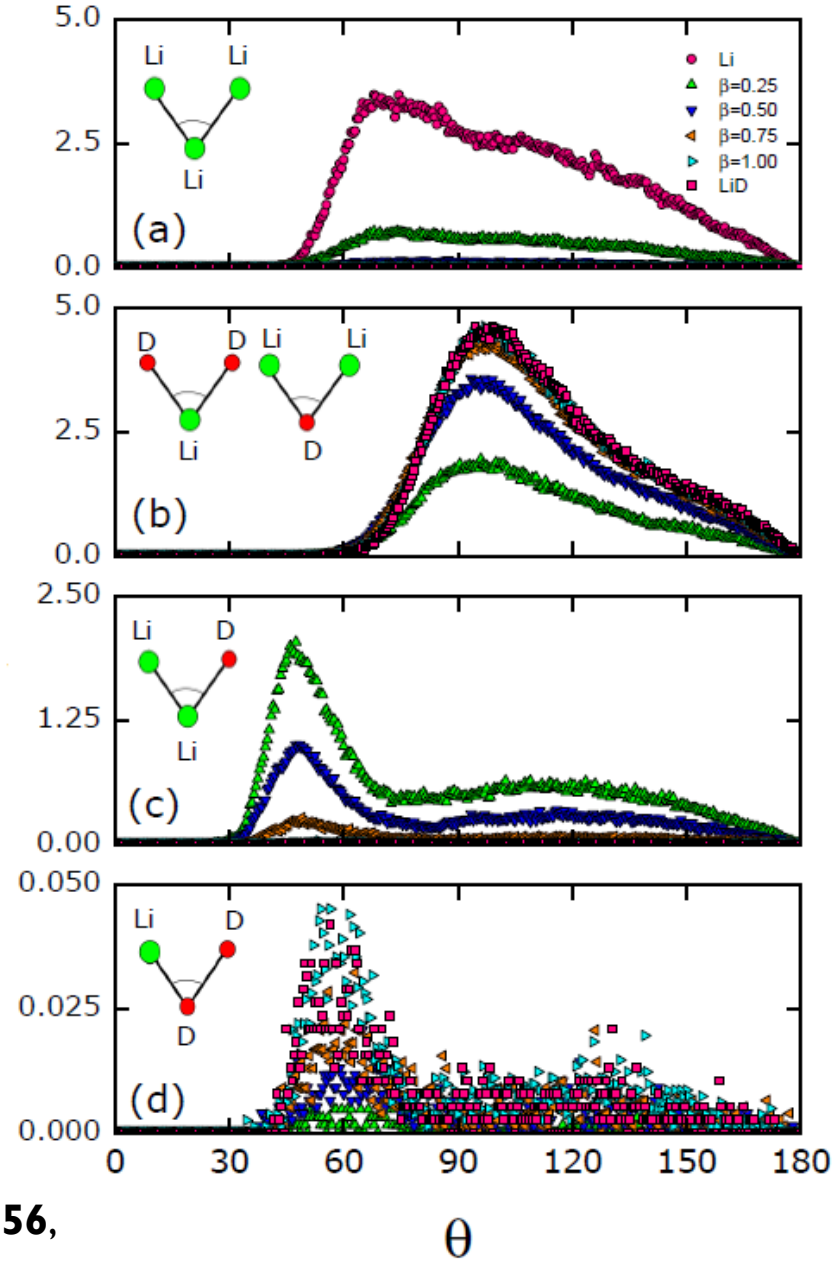

M. Chen, T. Abrams, M. Jaworski, E. A. Carter, *Nuclear Fusion,* **56**, 016020 (2016).

Liquid Li with inserted D atoms *below* the melting point of LiD

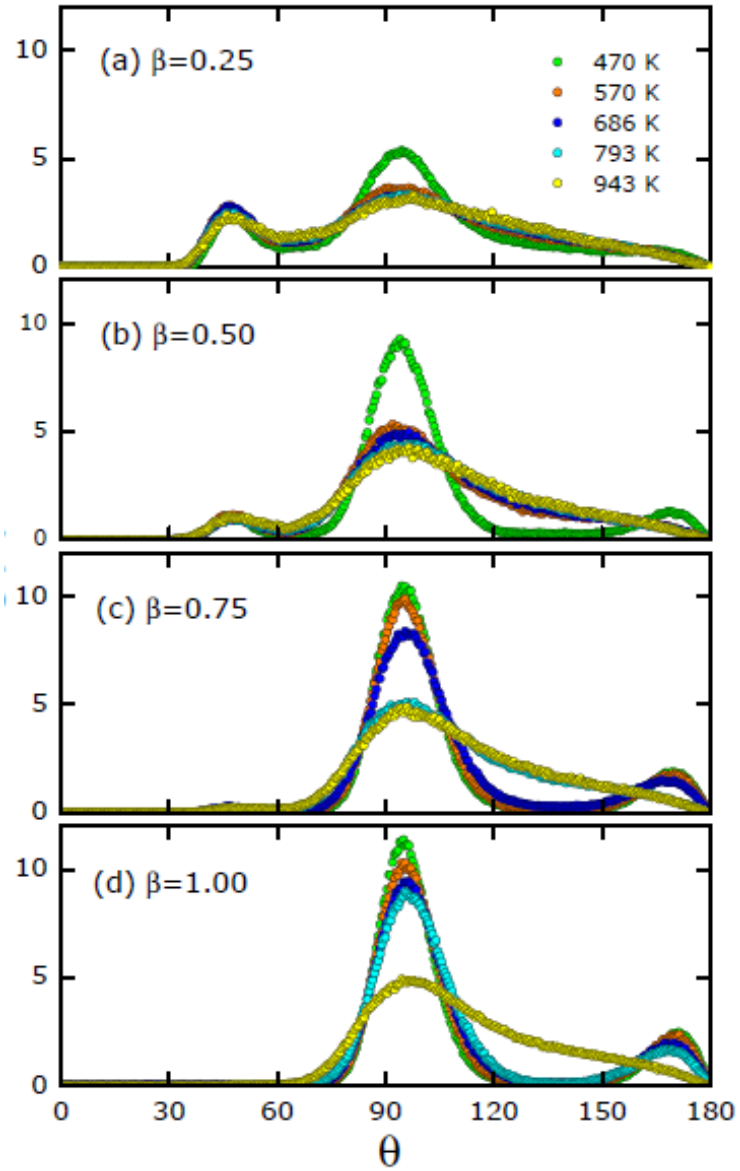

- **Above the melting point of Li (453 K).**
- **D atoms inserted into liquid Li randomly, without knowledge of rock-salt structure of LiD.**
- **At low β, coexistence of liquid Li and solid LiD.**
- ***Rock-salt LiD nuclei formed.***

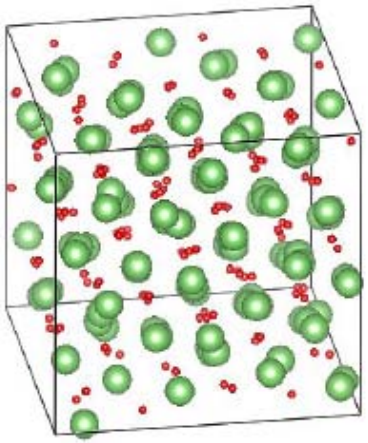

(d)
β=1.00, T=793 K

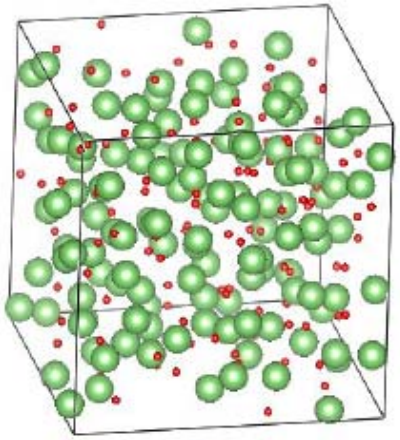

(h)
β=1.00, T=943 K

M. Chen, T. Abrams, M. Jaworski, E. A. Carter, *Nuclear Fusion,* **56**, 016020 (2016).

Temperature and Composition Dependent D and Li Diffusivities

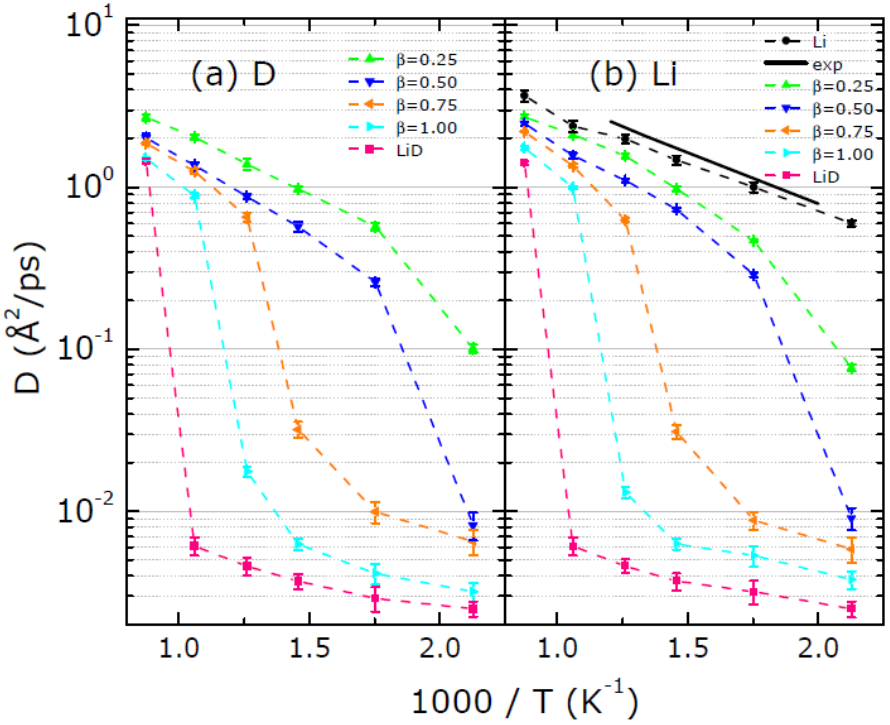

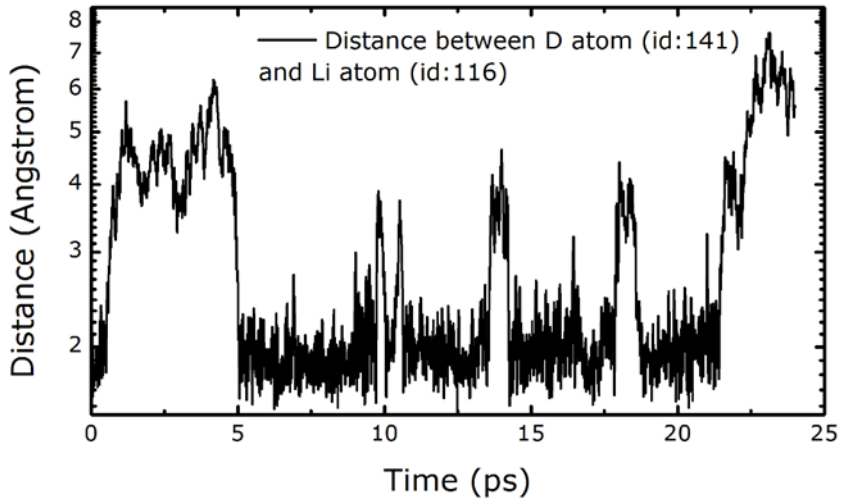

- **Validation: KSDFT-MD Li diffusivity in liquid Li matches experiment.**
- **Large changes in diffusivities caused by liquid-solid phase transitions.**
- **At lower temperatures, D and Li diffusivities are correlated, *suggesting chemical bonding.***

- **Diffusion coefficients of both Li and D lowered due to existence of LiD in liquid Li (chemical bonding traps both species).**
- **At high exposures to D, and at T < ~960K, predict form mix of solid LiD in liquid Li.**
- **Implies D sequestered in liquid Li.**
- **Design principle: keep D concentration sufficiently high to form solid LiD (higher T_{melt}) for improved thermal robustness of reactor wall.**

M. Chen, T. Abrams, M. Jaworski, E. A. Carter, *Nuclear Fusion*, **56**, 016020 (2016).

Characterization of Li-Mo Interfaces

- New Li-Mo MEAM force field fit to KS-DFT adsorption energies

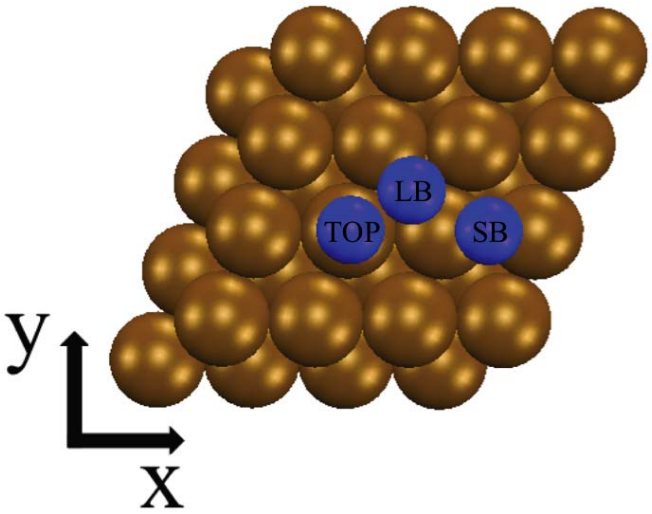

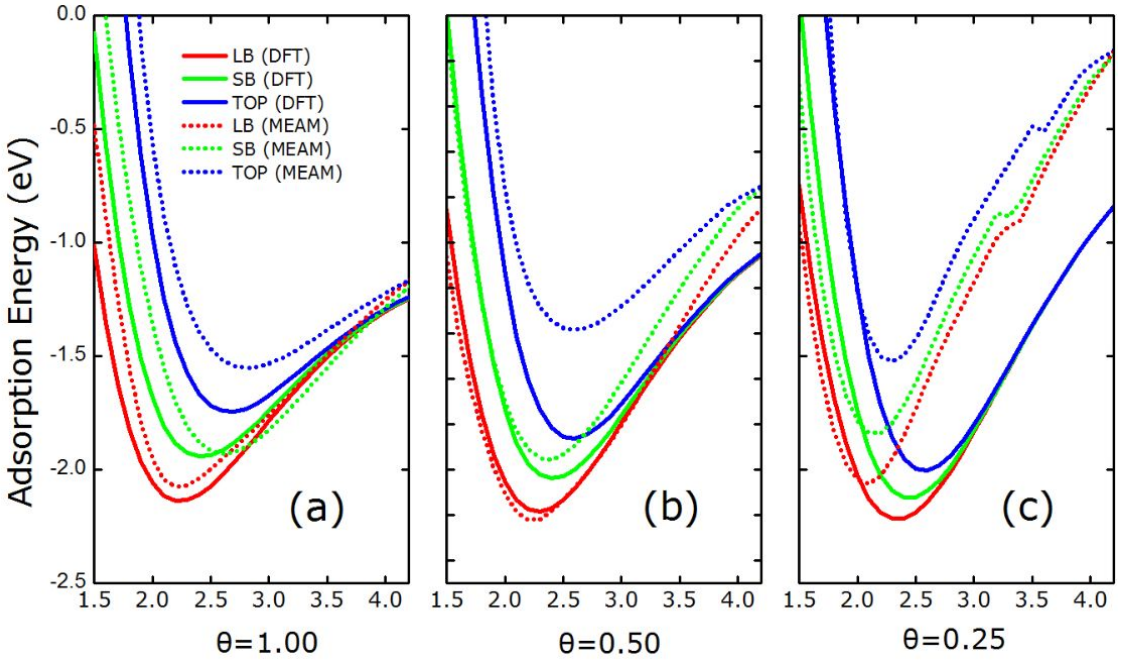

- KS-DFT predicts strongest binding of Li to Mo surface vacancies
- Explains TPD measurements
- Suggests roughened Mo substrates could enhance Li film adhesion

M. Chen, J. Roszell, et al. J. Phys. Chem. B **120**, 6110 (2016)
J. R. Vella, M. Chen, et al. Nucl. Fusion **57**, 116036 (2017)

3 ns KSDFT-Derived MEAM MD of Li Droplet on Clean Mo(110) at 460 K

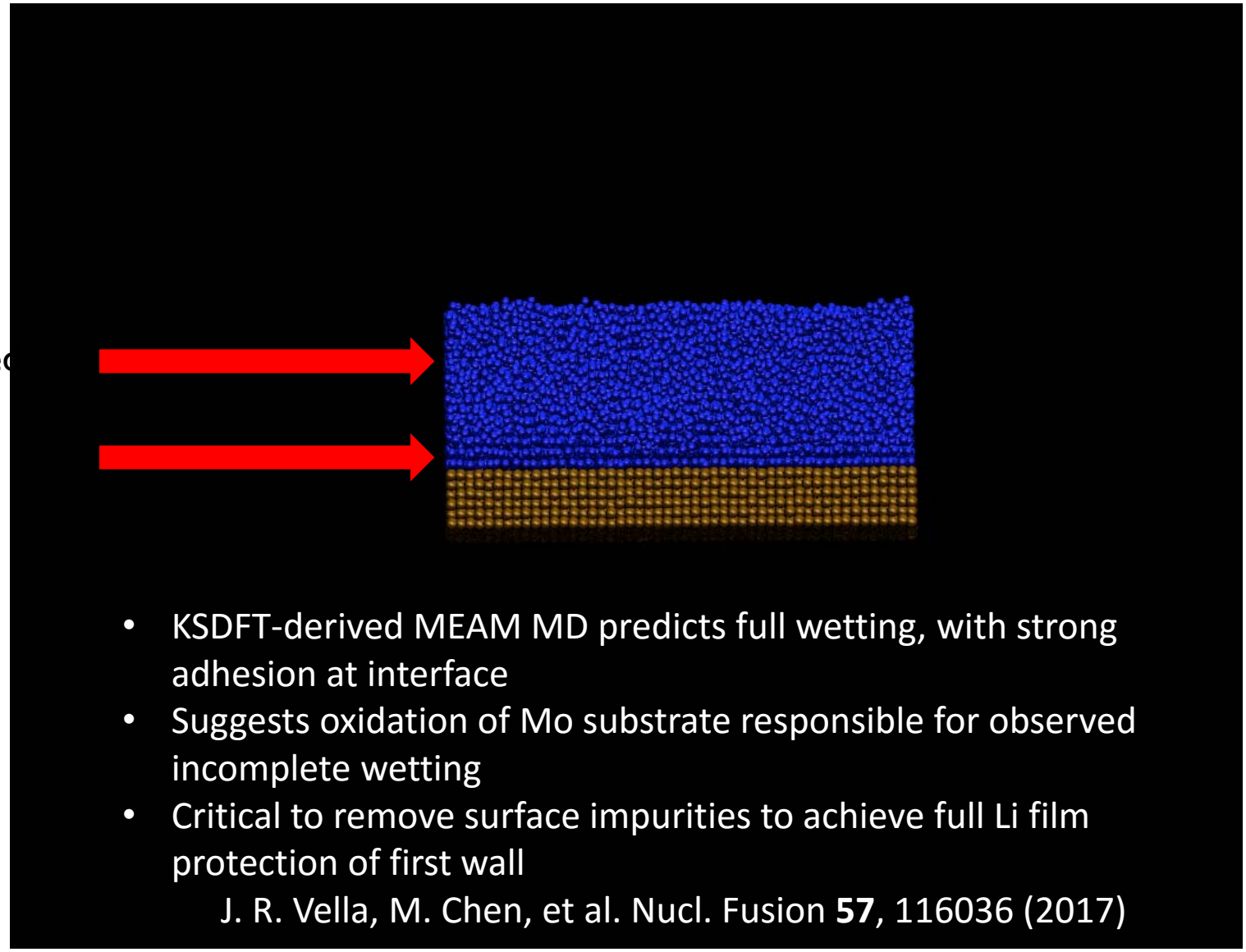

- KSDFT-derived MEAM MD predicts full wetting, with strong adhesion at interface
- Suggests oxidation of Mo substrate responsible for observed incomplete wetting
- Critical to remove surface impurities to achieve full Li film protection of first wall

J. R. Vella, M. Chen, et al. Nucl. Fusion **57**, 116036 (2017)

Conclusions

- Vacancies created by particle bombardment in W can absorb large amounts of D/T.
- Must keep W divertor at elevated temperature to anneal out vacancy-interstitial pairs and encourage D/T diffusion to and desorption from W surface.
- Evidence for LiD sequestration in liquid Li => origin of anomalously low sputtering.
- Keep liquid Li divertor saturated with D to operate at more practical temperatures for longer times.
- Sputter Mo substrate to roughen and remove oxygen to enhance liquid Li film adhesion.

Thanks

Dr. Donald Johnson
(→ Silicon Therapeutics)

Dr. Mohan Chen
(→ Temple U)

Chuck Witt

Experimental collaborators: Michael Jaworski and Tyler Abrams (PPPL)
John Roszell and Bruce Koel (Princeton CBE)

Classical Potential MD collaborators: Joey Vella, Thanos Panagiotopoulos, Pablo Debenedetti, Frank Stillinger (Princeton CBE)

$: DOE-FES, ONR